Hole Transport Materials based on Twisted Molecular Structure with a Single Aromatic Heterocyclic Core to Boost the Performance of Conventional Perovskite Solar Cells

Huiqiang Lu[a], Fei Wu,[*a] Yang Yang[a], Shufang Li[a], Yong Hua[*b], Linna Zhu[*a]

[a]*Chongqing Key Laboratory for Advanced Materials and Technologies of Clean Energy, School of Materials & Energy, Southwest University, Chongqing 400715, P.R. China.*

[b]*Yunnan Key Laboratory for Micro/Nano Materials & Technology, School of Materials and Energy, Yunnan University, Kunming 650091, Yunnan, P. R. China*

Corresponding Author: *Linna Zhu, School of Materials & Energy, Southwest University, Chongqing, China, E-mail address: lnzhu@swu.edu.cn. Tel.: +86 23 68254957.*

Fei Wu, School of Materials & Energy, Southwest University, Chongqing, China, E-mail address: feiwu610@swu.edu.cn.

Yong Hua, School of Materials and Energy, Yunnan University, Kunming, Yunnan, China, E-mail address: huayong@ynu.edu.cn.

Table of contents

1. General information

2. Synthetic procedures, NMR spectra and HRMS spectra

3. Density functional calculations

4. Photophysical properties

5. Cyclic voltammetry measurements

6. Thermal properties

7. X-ray diffraction (XRD) measurements

8. The Space-charge-limited current (SCLC) hole mobility measurements

9. Device materials, fabrication and testing

1. General information

Unless otherwise stated, all starting materials were purchased from commercial suppliers (Sigma Aldrich, and the Energy Chemical) and used without further purification. The nuclear magnetic resonance (NMR) spectra were obtained from a BRUKER AVANCE Ⅲ 600 MHz NMR Instrument (in $CDCl_3$). MALDI-TOF HRMS was performed on a Bruker Autoflex instrument, using 1,8,9-trihydroxyanthracene as a matrix. UV-vis absorption spectra were measured on a Shimadzu UV-2450 absorption spectrophotometer. Cyclic voltammetry (CV) test was performed on a CHI-660A in $CDCl_3$ under a nitrogen atmosphere, using a saturated calomel electrode (SCE) as a reference electrode and ferrocene as an internal standard. Thermal gravimetric analysis (TGA) was performed on a TGA Q50 at a heating rate of 10 °C min^{-1} under a nitrogen atmosphere. Differential scanning calorimetry (DSC) measurement was performed on a DSC Q20 instrument at a heating rate of 10 °C min^{-1} under a nitrogen atmosphere. The cross-sectional SEM image of the device was characterized by FE-SEM images (JSM-7800F). Atomic force microscopy (AFM) was used for characterizing the morphology using a CSPM5500. Water contact angles were measured on contact angle measurement apparatus JC2000D, Shanghai Zhongchen Digital Technology Co., Ltd., China. Steady-state PL spectra were recorded on Fluorolog®-3 fluorescence spectrometer (Horiba). Time-resolved PL decay curves were measured by a single photon counting spectrometer from Horiba Instruments (Fluorolog®-3) with a Picosecond Pulsed UV-LASTER (LASTER375) as the excitation source. The current–voltage (*J–V*) curves were measured under 100 mW cm^{-2} (AM 1.5 G) simulated sunlight using Keithley 2400 in conjunction with a Newport solar simulator (94043A). The external quantum efficiency (EQE) was calculated from the photocurrent measurement under

monochromatic illuminations at different wavelengths, using a 150 W xenon lamp and a monochromator.

2. Synthesis

Compound 1 and **2** were synthesized according to literature[1].

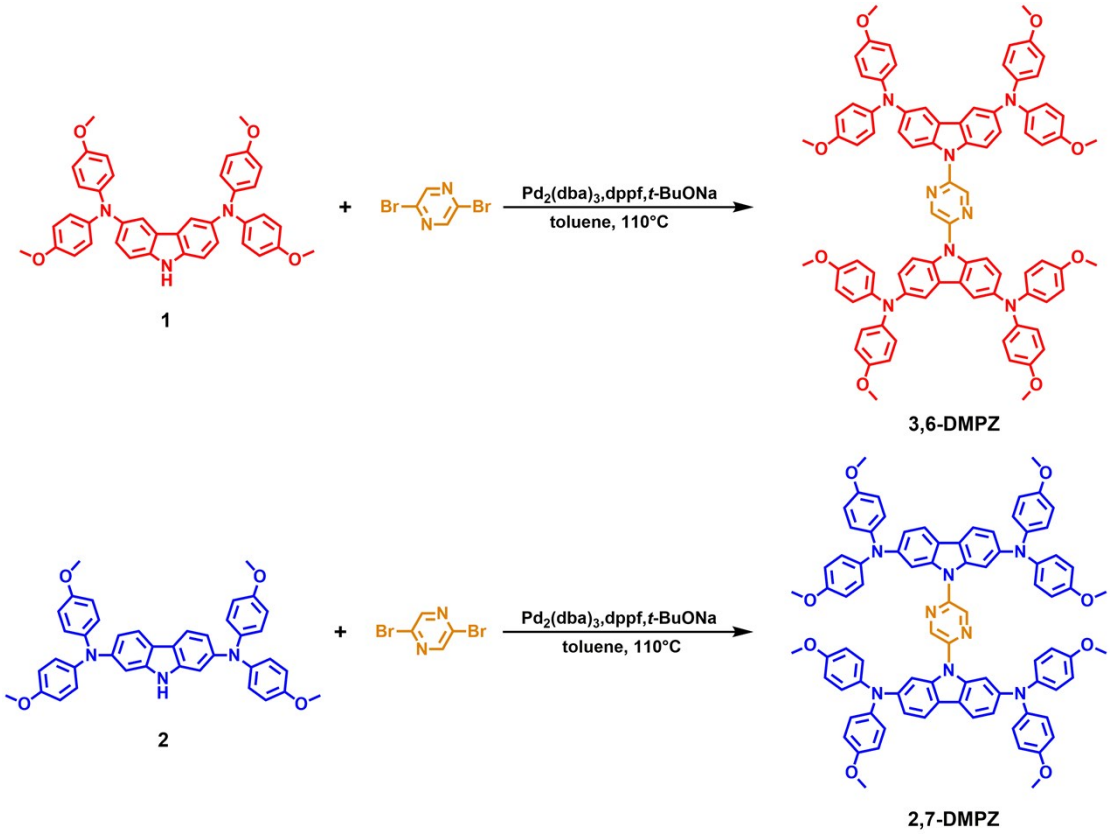

Scheme 1. The synthetic routes of 3, 6-DMPZ and 2, 7-DMPZ.

Synthesis of ***3,6-DMPZ*** **(9,9'-(pyrazine-2,5-diyl)bis(N^3,N^3,N^6,N^6-tetrakis(4-methoxyphenyl)-9*H*-carbazole-3,6-diamine)):** A mixture of 2,5-dibromopyrazine (100 mg, 0.42 mmol), compound 1 (652.8 mg, 1.05 mmol), $Pd_2(dba)_3$ (38.5 mg, 0.042 mmol), dppf (23.3 mg, 0.042 mmol) and *t*-BuONa (121.1 mg, 1.26 mmol) in anhydrous toluene (15 mL) was placed in a Schlenk tube under an Argon atmosphere and was stirred at 110 ℃ for 36 h. After cooling, the reaction was quenched by adding water, and then was extracted with dichloromethane. The organic layer was washed with brine and dried over anhydrous Na_2SO_4. After solvents were evaporated, the residue was purified

by column chromatography over silica gel using dichloromethane as the eluent to give the product (348.9 mg, 63%) as an orange solid. ^{1}H NMR (600 MHz, $CDCl_3$, ppm) δ 8.91 (s, 2H), 7.72 (d, *J* = 8.9 Hz, 4H), 7.54 (d, *J* = 1.7 Hz, 4H), 7.10 (d, *J* = 8.9, 4H), 6.93 (d, *J* = 8.9 Hz, 16H), 6.71 (d, *J* = 8.9 Hz, 16H), 3.70 (s, 24H). ^{13}C NMR (151 MHz, $CDCl_3$, ppm) δ 155.05, 145.04, 143.45, 142.21, 138.05, 135.42, 125.64, 124.88, 124.02, 115.64, 114.67, 111.91, 55.53. MALDI-TOF for $C_{84}H_{70}N_8O_8$ m/z: $[M]^+$ calcd 1318.5317; found 1318.5292.

Synthesis of ***2,7-DMPZ*** **(9,9'-(pyrazine-2,5-diyl)bis(*N*^{2},*N*^{2},*N*^{7},*N*^{7}-tetrakis(4-methoxyphenyl)-9*H*-carbazole-2,7-diamine)):** A mixture of 2,5-dibromopyrazine (100 mg, 0.42 mmol), compound 2 (652.8 mg, 1.05 mmol), $Pd_2(dba)_3$ (38.5 mg, 0.042 mmol), dppf (23.3 mg, 0.042 mmol) and *t*-BuONa (121.1 mg, 1.26 mmol) in anhydrous toluene (15 mL) was placed in a Schlenk tube under an Argon atmosphere and was stirred at 110 ℃ for 36 h. After cooling, the reaction was quenched by adding water, and then was extracted with dichloromethane. The organic layer was washed with brine and dried over anhydrous Na_2SO_4. After solvents were evaporated, the residue was purified by column chromatography over silica gel using dichloromethane as the eluent to give the product (376.6 mg, 68%) as an yellow solid. ^{1}H NMR (600 MHz, DMSO, ppm) δ 8.58 (s, 2H), 7.87 (d, *J* = 6.4 Hz, 4H), 7.31 (s, 4H), 6.92 (m, 16H), 6.84 – 6.72 (m, 20H), 3.67 (s, 24H). ^{13}C NMR (151 MHz, DMSO, ppm) δ 155.63, 146.90, 144.83, 141.32, 140.31, 138.20, 126.42, 125.95, 120.56, 119.08, 117.48, 115.20, 104.63, 55.62. MALDI-TOF for $C_{84}H_{70}N_8O_8$ m/z: $[M]^+$ calcd 1318.5311; found 1318.5329.

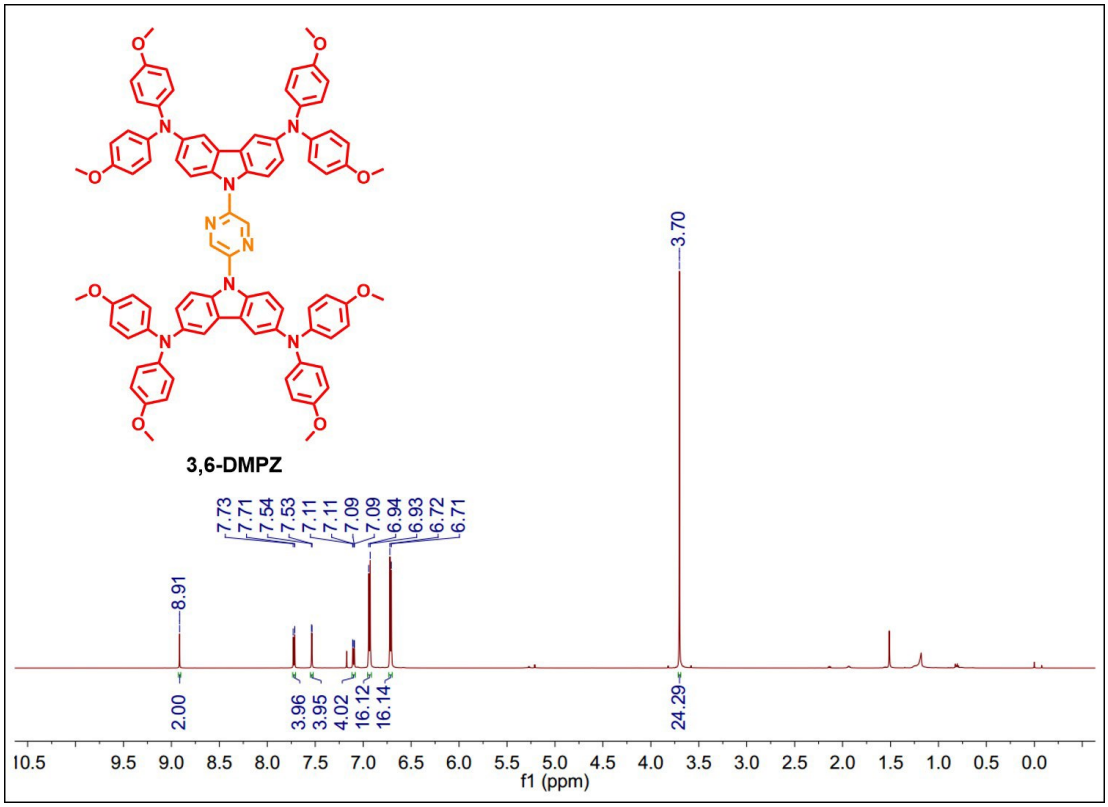

Fig. S1 ^{1}H NMR spectrum of 3, 6-DMPZ in $CDCl_3$

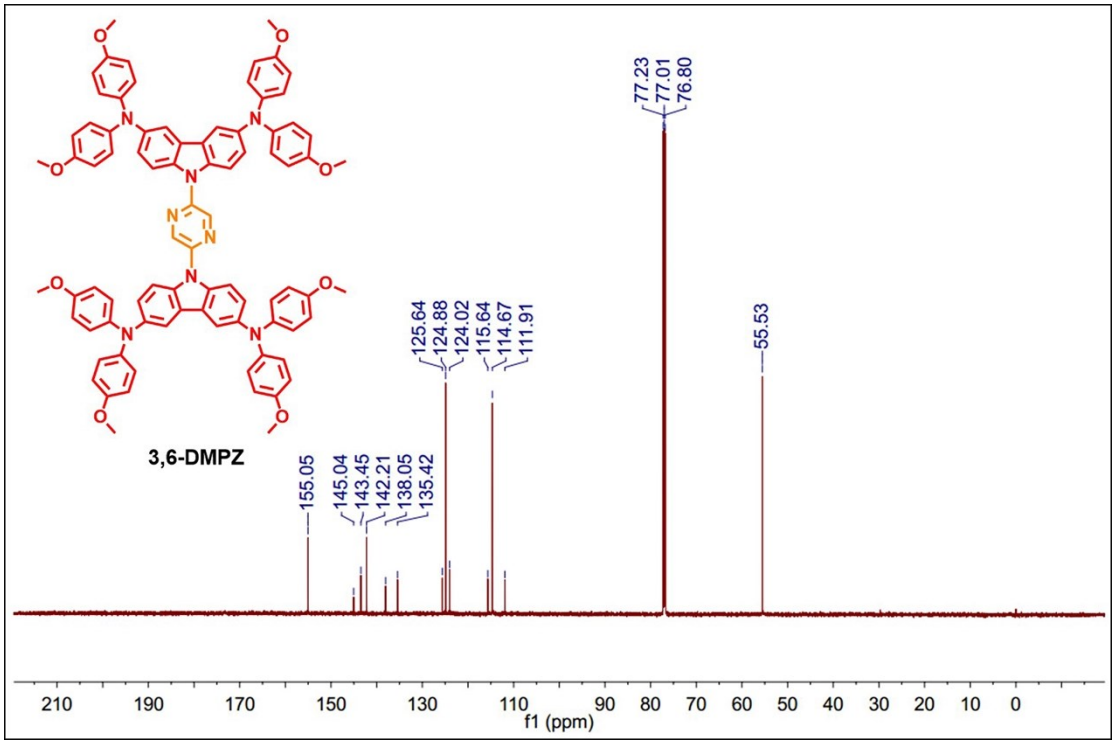

Fig. S2 ^{13}C NMR spectrum of 3, 6-DMPZ in $CDCl_3$

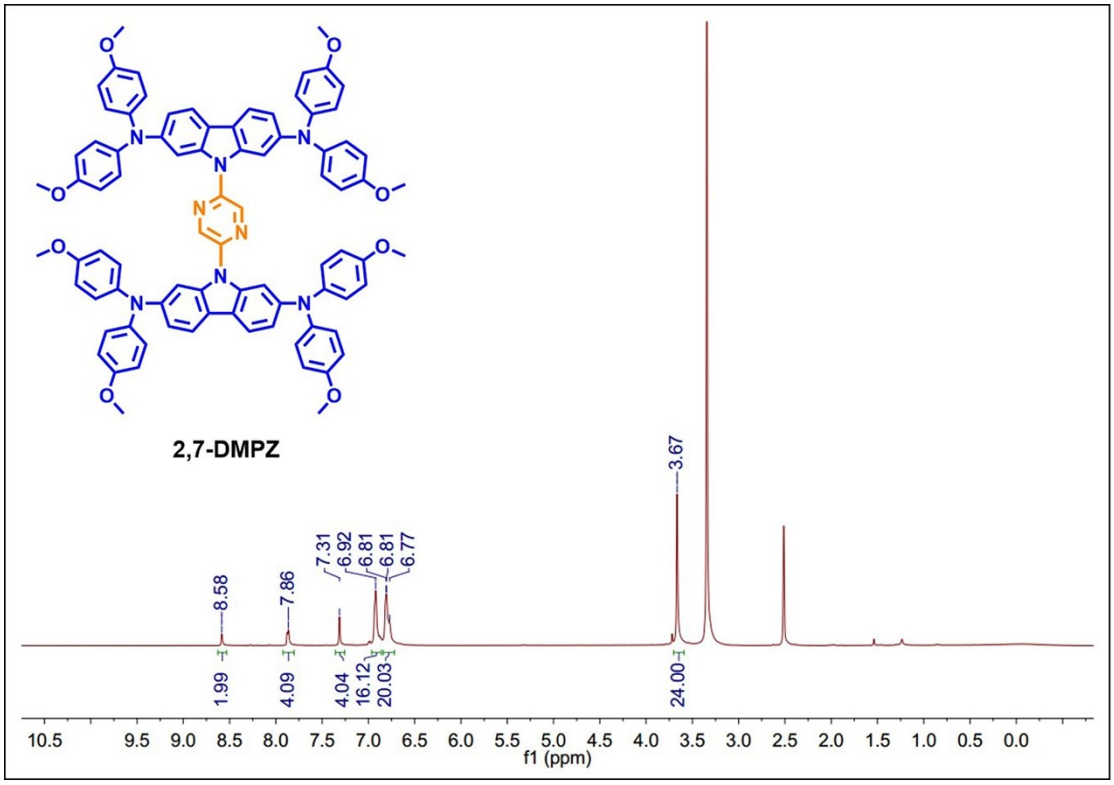

Fig. S3 ^{1}H NMR spectrum of 2, 7-DMPZ in DMSO-d_6.

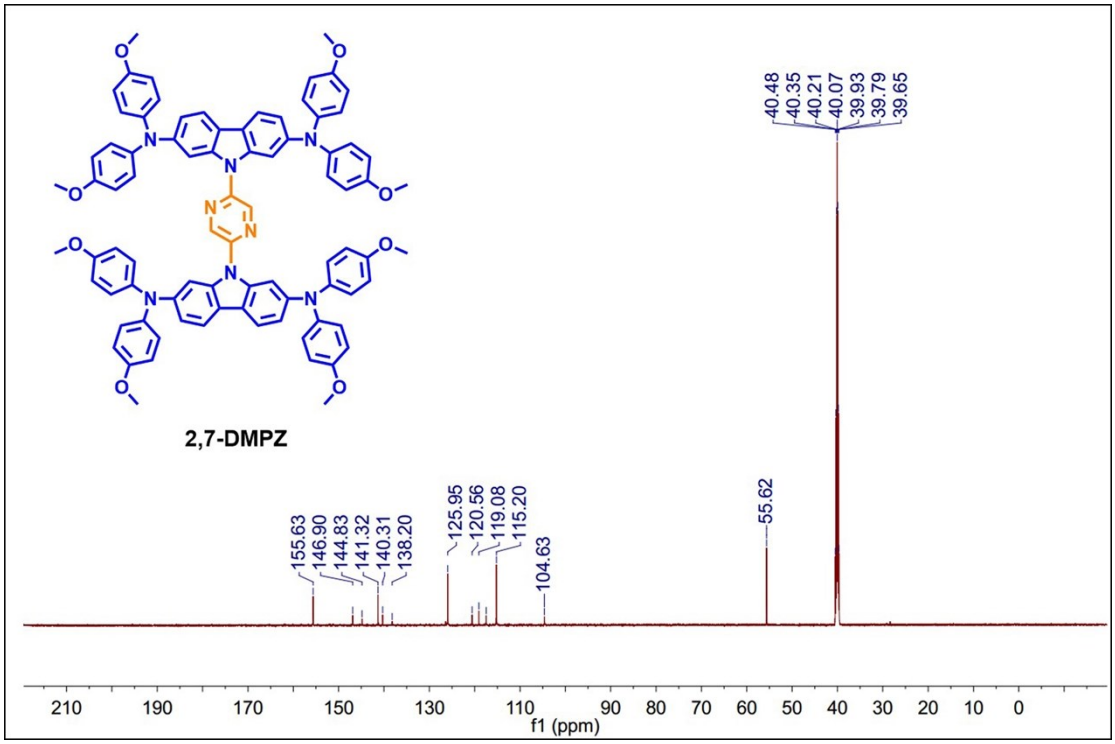

Fig. S4 ^{13}C NMR spectrum of 2, 7-DMPZ in DMSO-d_6

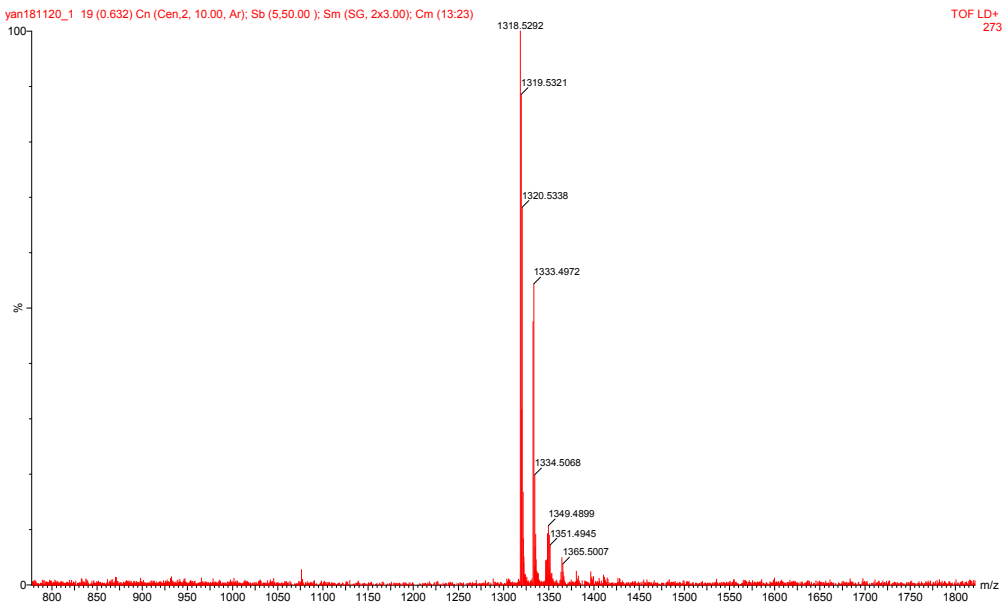

Fig. S5 MALDI-TOF mass spectrometry of 3, 6-DMPZ.

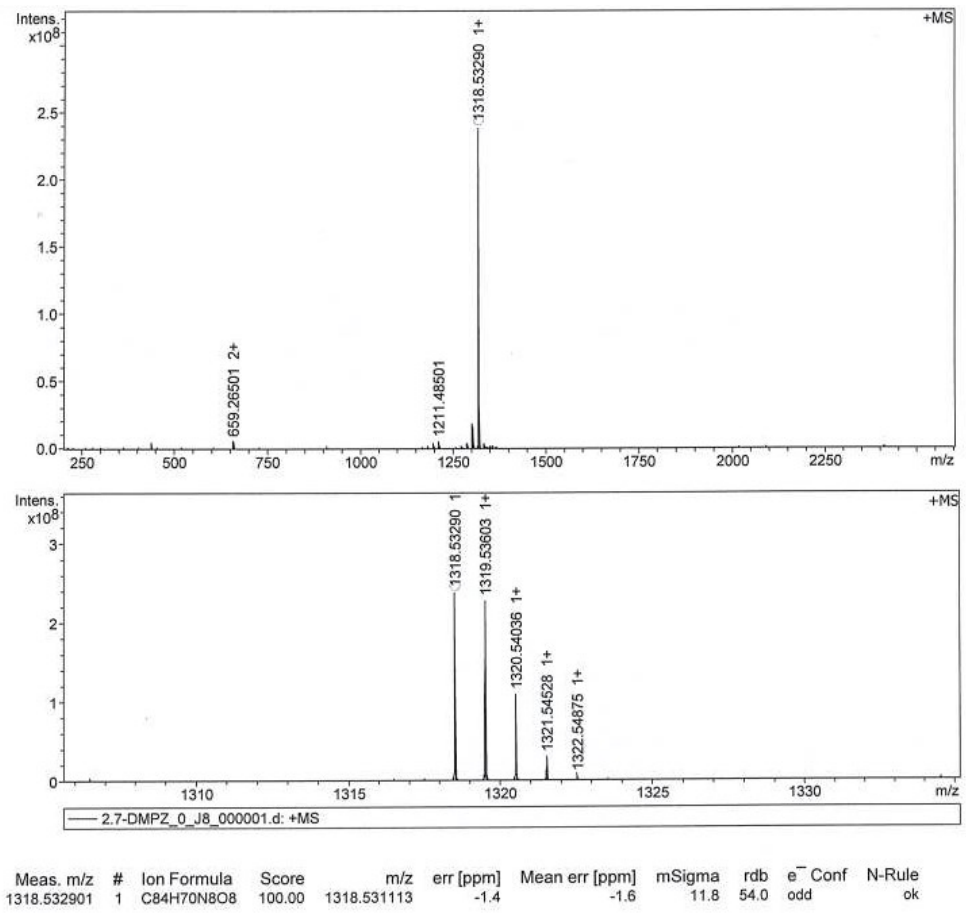

Meas. m/z	#	Ion Formula	Score	m/z	err [ppm]	Mean err [ppm]	mSigma	rdb	e⁻ Conf	N-Rule
1318.532901	1	C84H70N8O8	100.00	1318.531113	-1.4	-1.6	11.8	54.0	odd	ok

Fig. S6 MALDI-TOF mass spectrometry of 2, 7-DMPZ.

3. Density functional calculations

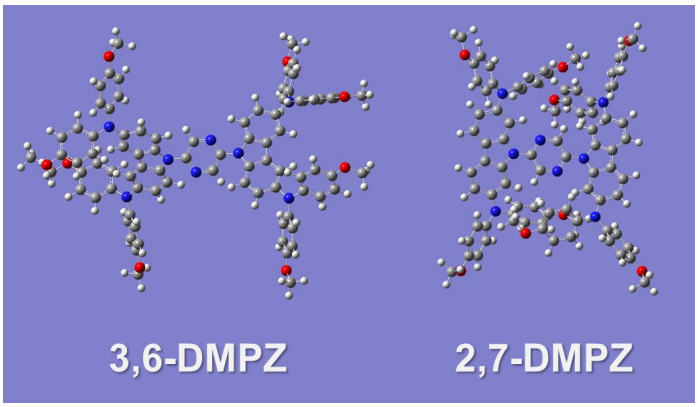

Fig. S7 DFT simulated molecule geometry of 3,6-DMPZ and 2,7-DMPZ.

4. Photophysical properties

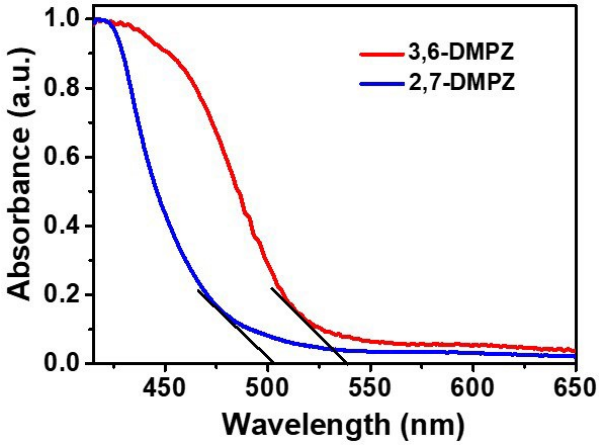

Fig. S8 UV-Vis spectrum of 3, 6-DMPZ and 2, 7-DMPZ films.

5. Cyclic voltammetry measurements

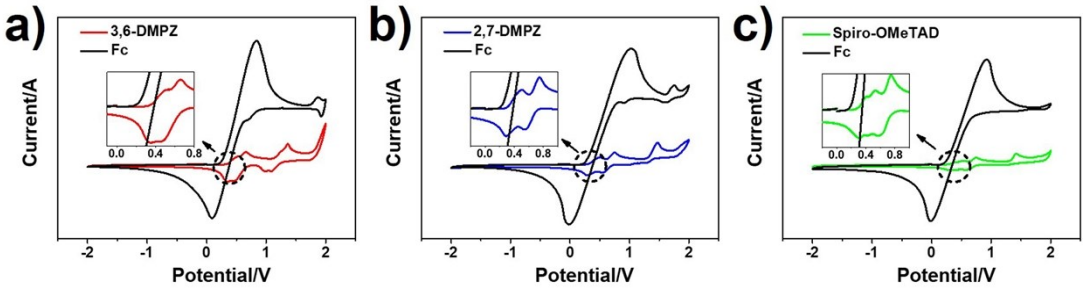

Fig. S9 CV curves of 3, 6-DMPZ and 2, 7-DMPZ together with spiro-OMeTAD.

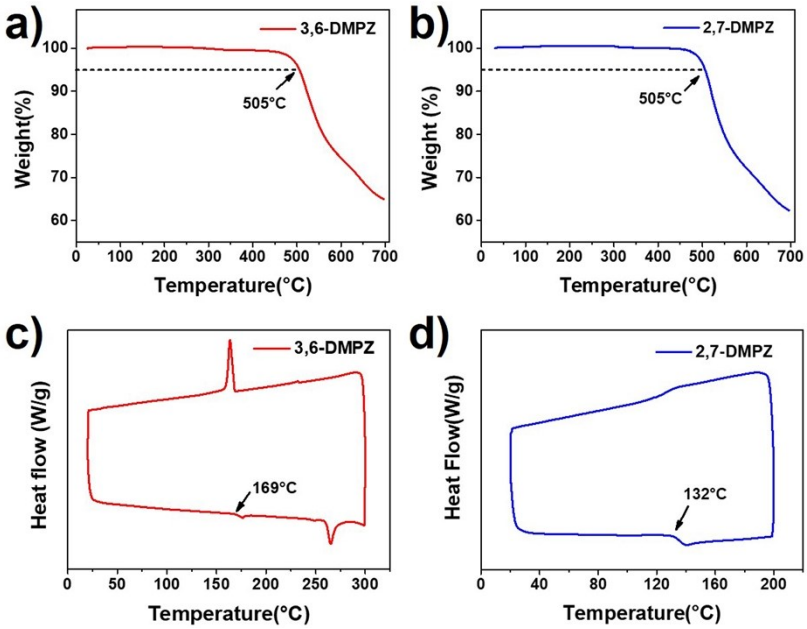

6. Thermal properties

Fig. S10 a), b) Thermogravimetric analysis (TGA) and c), d) Differential scanning calorimetry (DSC) of 3, 6-DMPZ and 2, 7-DMPZ under N_2 atmosphere.

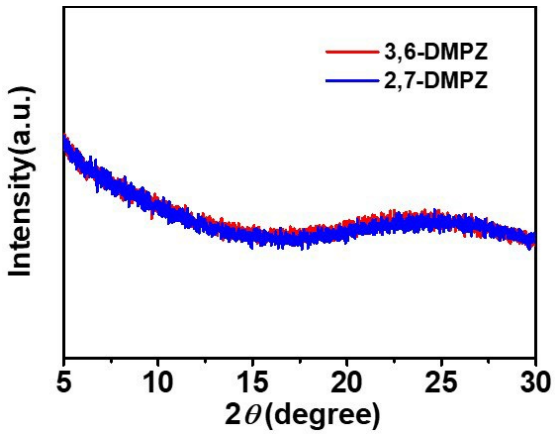

7. X-ray diffraction (XRD) measurements

Fig. S11 XRD diffractograms of 3, 6-DMPZ and 2, 7-DMPZ films.

8. The Space-charge-limited current (SCLC) hole mobility measurements

Hole mobility tests were conducted using a diode configuration of ITO/PEDOT:PSS/HTM/MoO_3/Ag by taking current-voltage current in the range of 0-6 V and fitting the results to a space charge limited form, based on the following equation $J = 9\varepsilon_\theta\varepsilon_\gamma\mu_h V^2/8L^3$. J is

the current density, L is the film thickness of the active layer, $\mu_h$is the hole mobility, ε_γ is the relative dielectric constant of the transport medium, ε_θ is the permittivity of free space ($8.85*10^{-12}$ F m^{-1}), V is the internal voltage of the device.

9. Device materials, fabrication and testing

Materials

In this work, all major materials were purchased from commercial suppliers and used without further purification, including PEDOT:PSS (Heraeus, Clevios PVP Al 4083), PbI_2 (*p*-OLED, >99.99 %), $PbCl_2$ (*p*-OLED, >99.99 %), MAI (*p*-OLED, ≥99.5 %), C_{60} (*p*-OLED, >99.5 %), Spiro-OMeTAD (*p*-OLED, ≥99.5 %), MoO_3 (Sigma-Aldrich, 99.97 %), DMF (Sigma-Aldrich, 99.8 %), DMSO (Sigma-Aldrich, 99.8 %), THF (J&K, 99.9%) and CB (Sigma-Aldrich, 99.8 %).

Device fabrication and testing

Preparation of HTM Solutions

As for the reference, the Spiro-OMeTAD solution was prepared according to the literature. To prepare the solution, 72.5 mg Sprio-OMeTAD was dissolved 1 mL chlorobenzene with 28.5 μL 4-tertbutylpyridine (*t*BP) and 17.5 μL lithium-bis(trifluoromethanesulfonyl)imide (Li-TFSI) stock solution (520 mg mL^{-1} in acetonitrile) as additives. Different HTMs (3,6-DMPZ and 2,7-DMPZ) were all dissolved in chlorobenzene with a concentration of 35 mg mL^{-1} and 50 mg mL^{-1}, with *t*BP and Li-TFSI as dopants.

Device fabrication

Devices were prepared on conductive fluorine-doped tin oxide (FTO) coated glass substrates. FTO-coated glass (14 Ω sq^{-1}) was cleaned by sequential sonication with a detergent solution, deionized water, ethanol, and acetone respectively. After washing by different solvents, the substrates were treated with oxygen plasma for two minutes before use. All the devices were fabricated based on

the conventional structure (FTO/compact TiO_2/Perovskite/HTM/Ag electrode). TiO_2 compact layer was fabricated by spin-coating the precursor solution (350 μL titanium isopropoxide and 25 μL HCl in 5 mL isopropanol) onto the FTO substrates at 5000 rpm for 60 s. Subsequently, the films were sintered on the hotplate at a temperature of 500℃ for 60 min (275 ℃ for 5 min, 325℃ for 5 min, 375℃ for 5 min, and 500 ℃ for 60 min). The perovskite film was deposited by spin-coating the precursor solution(The mole ratio of PbI_2:$PbCl_2$: MAI is 1:1:4, 202.8 mg PbI_2, 122.7 mg $PbCl_2$ and 279.8 mg MAI in 1 mL DMF) onto the TiO_2 substrate at 2000 rpm for 60 s, followed by annealing at 95 ℃ for 40 min in a nitrogen-filled glovebox. Then HTM was spin-coated on the top of the perovskite layer with a speed of 5000 rpm for 60 s. After oxidizing the HTM layer in the air for 15 h, a silver layer with a thickness of approximately 100 nm was deposited by thermal evaporation on the substrates to complete the devices.

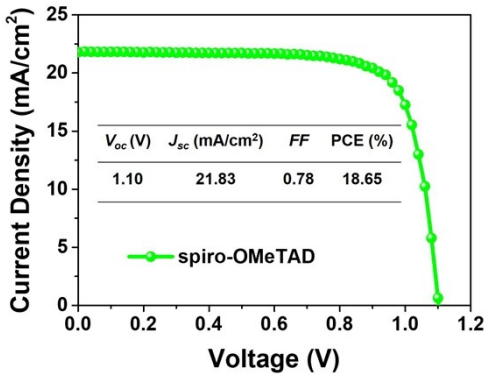

Fig. S12 *J–V* characteristics of the PSCs devices based on spiro-OMeTAD.

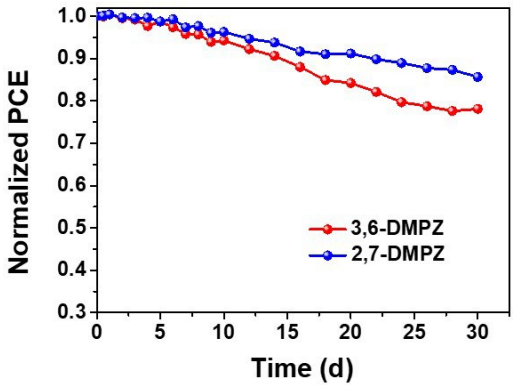

Fig. S13 Stability test of 3, 6-DMPZ and 2, 7-DMPZ based PSCs (unencapsulated) in N_2 atmosphere over 30 days.

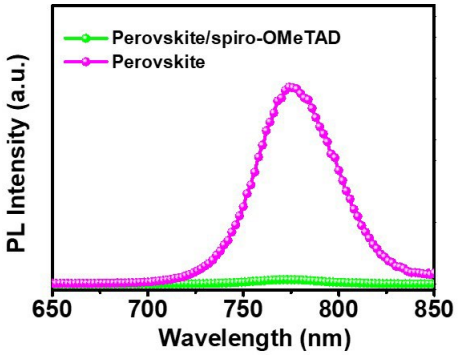

Fig. S14 Steady-state PL spectra of pristine perovskite film and that coated with spiro-OMeTAD on top.

Table S1. Photovoltaic parameters of perovskite solar cells using 3, 6-DMPZ and 2, 7-DMPZ as HTMs measured from forward scanning and reverse scanning

HTM	Scan Direction	V_{oc}(V)	J_{sc}(mA/cm^2)	*FF*	PCE (%)
3,6-DMPZ	forward	1.01	21.59	0.78	17.09
	reverse	0.99	21.55	0.74	15.77
2,7-DMPZ	forward	1.08	22.61	0.80	19.61
	reverse	1.06	22.58	0.79	18.86

Reference

1. F. Wu, Y. H. Shan, J. H. Qiao, C. Zhong, R. Wang, Q. L. Song and L. N. Zhu, *Chemsuschem*, 2017, **10**, 3833-3838.